Research Article

Luis Norberto López de Lacalle*, Gorka Urbicain Pelayo, Asier Fernández-Valdivielso, Alvaro Alvarez, and Haizea González

Wear-dependent specific coefficients in a mechanistic model for turning of nickel-based superalloy with ceramic tools

https://doi.org/10.1515/eng-2017-0024
Received April 24, 2017; accepted June 21, 2017

Abstract: Difficult to cut materials such as nickel and titanium alloys are used in the aeronautical industry, the former alloys due to its heat-resistant behavior and the latter for the low weight - high strength ratio. Ceramic tools made out alumina with reinforce SiC whiskers are a choice in turning for roughing and semifinishing workpiece stages. Wear rate is high in the machining of these alloys, and consequently cutting forces tends to increase along one operation.

This paper establishes the cutting force relation between work-piece and tool in the turning of such difficult-to-cut alloys by means of a mechanistic cutting force model that considers the tool wear effect. The cutting force model demonstrates the force sensitivity to the cutting engagement parameters (a_p, f) when using ceramic inserts and wear is considered.

Wear is introduced through a cutting time factor, being useful in real conditions taking into account that wear quickly appears in alloys machining. A good accuracy in the cutting force model coefficients is the key issue for an accurate prediction of turning forces, which could be used as criteria for tool replacement or as input for chatter or other models.

Keywords: Inconel 718, ceramics, cutting coefficients, time-dependent wear

***Corresponding Author: Luis Norberto López de Lacalle:** University of the Basque Country UPV/EHU, Department of mechanical engineering; Email: norberto.lzlacalle@ehu.eus, Tel: +34-946014216
Gorka Urbicain Pelayo, Asier Fernández-Valdivielso, Alvaro Alvarez, Haizea González: University of the Basque Country UPV/EHU, Department of mechanical engineering

1 Introduction

Gas and aero turbines manufacturing is a top notch application, in which machining plays an important role, being responsible for the final part precision and surface integrity. The use of new advanced materials has played a major role on this improvement; hence, up to 50% of the increase obtained in turbines efficiency is attributed to super alloys (nickel base) and titanium alloys, both kinds included in the group S (orange) in the ISO (513:2012) materials classification. The development of nickel-based superalloys led into an increase in the turbine entrance temperature up to 350°C over the last decades, and thus during the next years an increase of 200°C in the entrance temperature is estimated, based on Clean Sky European initiative [1, 2]. In manufacturing of turbines, turning is the most important operation for cases and disks for all kind of engine segments. Alloy Inconel 718 (UNS N07718) is by far the most widely used nickel-based superalloy and the most studied one. The high ramp up of new deliveries required by aeroengine market implies an increase in cutting speed, that can be provided by ceramic tools.

Alloy 718 includes nickel as main element, being more than half of its mass by weight. It also has important quantities of chromium and iron, around 19% wt. and other non-insignificant quantities of alloying elements such as niobium, molybdenum, titanium or aluminum. Turbine vases and discs represent the principal component made of Alloy 718 as high-strength is required at high temperatures given the high centrifugal force reached by engine disks running at full load, but it is also used in cases, parts of combustor, blades, etc. This alloy maintains high strength and good ductility up to about 650°C. For many workshops, it is the reference of the group S material regarding machinability

However, these alloys are also difficult-to-cut materials (*i.e.*, the present high specific cutting force, rapid tool wear) because of their tendency to suffer work hardening by the tooltip rubbing effect on just machine surface on

one hand, and their high shear strength and ductility on the other. In addition, the highly abrasive nature of the alloy carbide particles reduces tool life and produces poor surface finish. Because of that, the thermo-mechanical and metallurgical phenomena between tool insert and machined surface need to be explored. That fact explains the efforts done in the last years on this issue. A time ago, Narutaki *et al.* [3] studied the wear resistance of several ceramic tools during severe turning conditions up to 500 m/min. A complete state of the art in the field of ceramics and Inconel 718 machining can be found in Dudzinski *et al.* [4], in which wear evolution was also considered. In order to define appropriate tool geometry and cutting conditions for such difficult to cut materials, intense research work under the concept of high speed machining (HSM) was performed, employing carbide tools in the turning process. Hence, Fang and Wu [5] explained a detailed comparative machining study between Inconel 718 and Ti-6Al-4V, finding empirical relationships to determine cutting forces depending on cutting speed and feedrate. Additionally, Thakur *et al.* [6] studied tool wear effect and showed the trends in the surface finish under different cutting conditions.

On the other hand, and referring to ceramic tools, the so-called hard turning technique of hardened steel was studied. Hard turning in automotive applications must be stable, so statistical analysis of previous results is a valuable approach; so, Khotamasu *et al.* [7] presented a model to predict cutting tool flank wear and forces in hard turning based on experimental data; in addition, Kountanya [8] developed a general 3D model for corner-radiuses, chamfered, edge-honed cutting worn tool. Some industrial applications of hard turning are found in [8–10], in which wear evolution dramatically affects both part quality and process economy; tool wear causes higher forces and temperatures, affecting quality. Hard turning presents two choices, the expensive PCBN tools on one hand and the cheaper ceramic tool approach on the other. The best option in ceramic tool involves the use of hard ceramic matrix (Al_2O_3) reinforced with extremely resistant silicon-carbide whiskers. This type of ceramic inserts is able to withstand 2000°C, providing the whiskers enough toughness for interrupted turning. The growing requirement to increase productivity, along with the interest for reducing coolant consumption during machining of nickel-base alloys, has turned attention to ceramic tools, which are able to withstand the high temperatures reached during the machining of Fe-Ni based alloys, and making the dry cutting approach feasible. In this issue, several authors investigated, such as Arunachalam *et al.* [11] who analyzed the CBN and mixed ceramic (Al2O3 and TiC) tools behaviour using optimal cutting parameters [12], observing the residual stresses and surface integrity of workpieces. In [13] it is studied the ceramic tool failure in intermittent hard turning, proposing a method to stablish stresses along cutting length. Cermets were also under evaluation by Xu *et al.* [14] at cutting speed of 50 m/min, speed lower than ceramic values usually in the range of 300-400 m/min.

Regarding carbide tools, a practical view is shown in [15], focusing on the effect of excessively worn tools in nickel-based superalloys. Also, in [16], the effect of carbide size and spacing on the fretting wear resistance of Inconel 690 in experiments is presented, in the same way that Mi *et al.* [17] did. Fernández-Valdivielso *et al.* [18] identified as well the best combination of carbide grades, chipbreakers shapes, and other features for having the best tool performance. Additionally, they checked surface integrity effects.

High pressure cooling strategies help in turning process due to its ability to form an hydraulic wedge on tool rake face, lifting the chip and gain access to the cutting zone, which leads to a reduction of the tool-workpiece contact region lowering the friction zone, which in turn results in reduction in cutting temperature and component forces. This phenomenon was observed by Ezugwu and Bonney [19], who machined Alloy 718 with carbide tools at speeds up to 50 m/min using conventional and high coolant pressures, up to 203 bar. Vagnorius and Sørby [20] claimed that SiAlON ceramic inserts with improved resistance to notching in machining of Alloy 718 under high-pressure cooling comparing it with conventional one. They observed that notch wear increased but it was not critical to tool live, and even flank wear was reduced. Wei *et al.* [21] studied flank wear and the influence of hydrogen contents on the rake crater wear in Ti-alloys. Other aeronautic alloys have been tested in terms of surface finish and residual stresses, such as Jomaa *et al.* [22] in dry machining conditions. Finally, other emerging approaches such as plasma or laser assisted processes [23], or ultrasonic assisted processes [2] are in discussion, being surface integrity always a concern.

In this study, straight cylindrical turning experiments were carried out in Inconel 718 using ceramic inserts to obtain specific cutting force coefficients. Face turning could be also an option, but operational performing is longer [24]. Other works focused on polycrystalline diamond (PCD) tools instead of ceramics [25] are also an interesting alternative, but temperature is always a serious drawback for PCD. Testing is necessary to study the complex tool wear in turning of such a low machinability material. Starting from this experimental base, the effects of

depth of cut and cutting speed on tool flank wear were also investigated.

The model can be used to determine forces on turning of thin-walled cases or other turbine components, or being part of a chatter model.

2 Force Modelling

Similar in essence to other predictive models in turning and milling [26, 27], a mechanistic model is proposed for calculating turning force. But, here an additional component is considered. So, the total force during the cutting process is divided into two main components. Firstly, cutting force components due to the chip removal process itself, which it is supposed to remain steady along the process. Secondly, a component related with the tool wear growing along the cutting process, which the novelty of the model. The latter component depends on wear and consequently on machining time, so it must time-dependent, as it is shown in the Equation (1) for modelling the total force during the chip removal process.

$$F(t) = F_{cutting} + F_{wear}(t) \tag{1}$$

At the same time, the so-called cutting force is subdivided into two effects: the force due to the shear stress, F_c, which is the dominant component of the removal process and responsible of the great fraction of the energy consumption. And secondly, the edge force F_e at the rake and relief surfaces, due to the friction contact between the chip and the tool insert produced during chip removal and some from the rubbing of relief face on part surface. If those three effects are decomposed, the equation results as follows:

$$F(t) = F_c + F_e + F_c(t) \tag{2}$$

The wear component allows adapting this model to the full process time, up to flank wear reaches the maximum threshold, usually V_B 0.3 mm is the ISO recommendation is followed. The models for each of the three subcomponents are as follows.

2.1 Shear force component

The shear force F_c comes from the metal cutting process itself, involving the shear deformation process inherent to chip formation in ductile alloys. Using a linear model, and introducing the effects of the side cutting edge angle and the depth of cut (a_p) inside the cutting coefficient, cutting force can be expressed as a function of the feed. The approach includes the effect of hardening in the coefficient dependency on a_p. Equation (3) shows the model for the coefficient and force component [28]:

$$F_{cx}(ap) = K_{cx}(ap) \cdot f \tag{3}$$

where K_{cx} is the cutting coefficient for the X direction in [N/m] considering the depth of cut inside the cutting coeffcient, a_p the depth of cut and f the feed per revolution. Similar relationships are established for the Y and Z directions.

2.2 Edge force component

The interaction between the workpiece surface and the tool flank face is still not well understood. From the works of Kobayashi and Thomsen [29], along with Thomsen *et al.* [30] and Zorev [31], it can be said that the deformation located in the primary shear zone and the friction phenomena on the rake face are not mainly affected by flank wear, that is, the basic cutting quantities remain unaffected by the tool flank wear land size.

The edge force is considered as the friction, adhesion and diffusion phenomena over the chip-rake face, and it can be written as in [28]:

$$F_{ex}(ap) = K_{ex}(ap) \tag{4}$$

where K_{ex} is the corrected specific edge force in X direction in [N], one that depth of cut is introduced. Similar relationships are found in Y and Z directions.

2.3 Wear force component

As it was explained in the previous subsection, flank wear has several consequences on process. For instance, it tends to stabilize the system mainly at low spindle speeds: this is the so-called process damping effect, very known in study of the chatter vibration problem. On the other hand, cutting becomes more aggressive with cutting edge dullness and forces increase.

Two main different research lines were used to model the effect of the tool flank wear. The first approach based on the contact force model [32, 33] establishes a proportionality relationship between the contact force and the displaced volume of the workpiece under the tool. This model is suitable for mild steels turning, but not for hard materials because of the difficulty in estimating the displaced volume in short tool life spans. Besides, the mea-

surement of the flank wear length (V_B) becomes complicated for ceramic inserts, where cutting is so aggressive that tool life is short and chipping frequent.

The other proposed approach is based on the slip-line model [34]. In this concept, the frictional force originated by the sliding of a hard relatively smooth surface over a softer one can be assumed as the force needed to push layers of plastically deformed material along the soft surface ahead of asperities on the hard surface. So, Kobayashi and Thomsen considered the slip-line field under the tool flank wear. In the same way Waldorf *et al.* [35] introduced non-uniform load distribution along the flank wear area to estimate the ploughing force.

In this work, an alternative view of the edge wear is put into practice for the prediction of the total force. The method lies basically in the fact that it does not include any considerations onto the tool-workpiece material interaction, introducing them by means of coefficients. As the forces involved during machining of low-machinability materials are strongly time-dependent, even more if using ceramics tools (because of the high cutting speeds in excess of 300 m/min), it seems reasonable as a first approach an expression like Eq. (5):

$$F_{wx}(t) = K_{wx}(ap)\frac{V_c}{V_f}t \tag{5}$$

where K_{wx} is the specific edge force in X direction as function of the depth of cut. Further on, the physical sense and composition of this coefficient will be explained. The formula (5) also shows a ploughing force proportional to the chip removal speed given by the cutting speed and an inversely proportional dependence on the linear feed rate V_f given in mm/min.

3 Experimental setup and data acquisition

The straight turning experiments were conducted in a CMZ® TBI-450MC turning center, see Figure 1. The workpiece was a cylinder of Inconel 718 (⌀100 mm X L300 mm) in annealed state, clamped in a power chuck, important at high speeds, and using a tailstock. Dry condition was used because of ceramics resistance to heat, although MQL and cryogenic gases also have lead to good results [36]. Figure 1. Also shows the Cartesian coordinate system: the mean tangential cutting force (parallel to cutting speed), Z direction (workpiece axis) and Y axis, the radial direction.

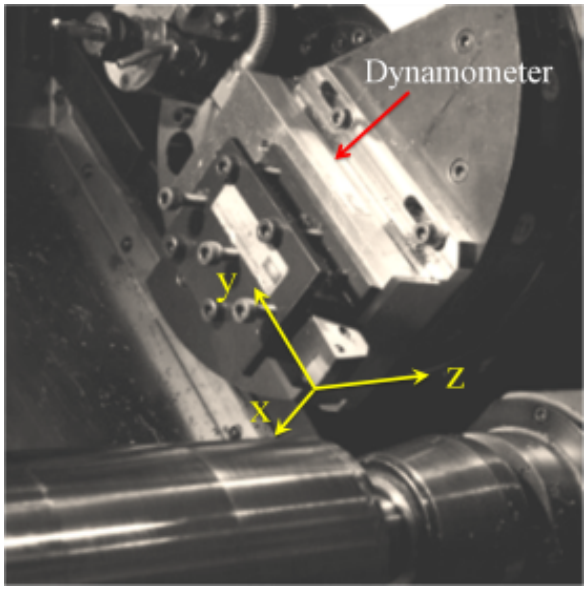

Figure 1: Experimental setup. turning workspace with dynamometer.

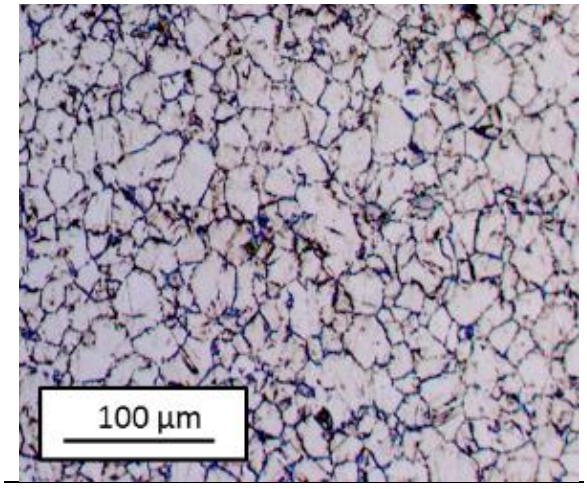

Figure 2: ASTM grain size near 8.

Alloy 718 is a Nickel-Chromium alloy, this 718 batch containing 53.60% of Ni and 18.30% of Cr. There are other important constituents as 18.02% Fe or important alloying elements, *e.g.* Mo 3.06%, Al 0.49%, Ti 0.98% or Nb+Ta 5.02%.

Studying wear when machining Inconel with ceramic tools is difficult because of the extremely aggressive nature of this material. This leads to very different results even when machining theoretically the same material with the same tool. So, material from a single batch was used for all tests to prevent any additional effect from chemistry or metallurgical variations. Specimen grain size was ASTM 8-9, microstructure on Figure 2.

Rhombic ceramic inserts supplied by NTK® Cutting Tools with ISO reference CNGN120708 T00520 WA1. The insert grade was a whisker-reinforced composite ceramic material with silicon-carbide whisker added to alumina (Al2O3+SiC: Density: 3.7 g/cm3; Hardness: 94.5 HRA; Bending Strength: 1200 MPa; Young modulus: 400 GPa, Thermal expansion coefficient: 7.0x1-6/K; Thermal conductivity: 35 W/mK).

The recording system used was composed by a KISTLER® dynamometer, type 9257B and a signal amplifier 5017, using an OROS® multichannel analyzer by NV-GATE software 6.2 and a PC for data processing and storage.

Cutting tests were done at two cutting speeds: Vc = 250 and 300 m/min, applying six different depths of cut: a_p ranging from 0.4 to 0.9 mm, in steps of 0.1 mm. Finally, four different feedrates were tested for each of the depths of cut, thus f = 0.05, 0.1, 0.15, 0.2 mm/rev.

Each of the series was driven with new inserts, being the wear measured at the end of each cutting experiment. All tests were repeated twice, and values were just the average one of both. If divergence between same tests were in excess of 7%, a third one was repeated in order to disregard the previous biased one.

4 Cutting force analysis

A typical turning force measurement is shown in Figure 3. In order to capture only the effect of cutting process and eliminating the tool wear effect, the force magnitude was measured at seven points/times for each experiment, along with the beginning of the first feed rate, and in the transition point between two different feed rates.

In this way, the forces due cutting process under each feed rate can be defined as:

$$\begin{aligned} F_{f=0.05} &= F1 \\ F_{f=0.10} &= F_{f=0.05} + \Delta 1 \\ F_{f=0.15} &= F_{f=0.10} + \Delta 2 \\ F_{f=0.20} &= F_{f=0.15} + \Delta 3 \end{aligned} \tag{6}$$

Following the above criterion, the force components due to the cutting process show the trend represented in the left side of Figure 4. For the subsequent analysis of the measured forces, a linear regression was carried out at each depth of cut under the four different feed rates adopting the form:

$$F = K_c \cdot f + K_e \tag{7}$$

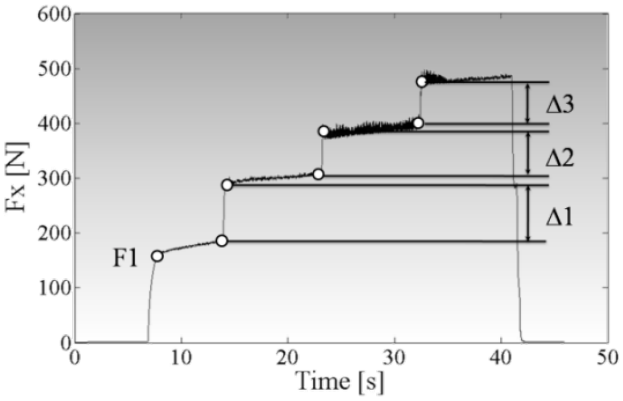

Figure 3: Example of a single direction signal force measurement using four different feed rates.

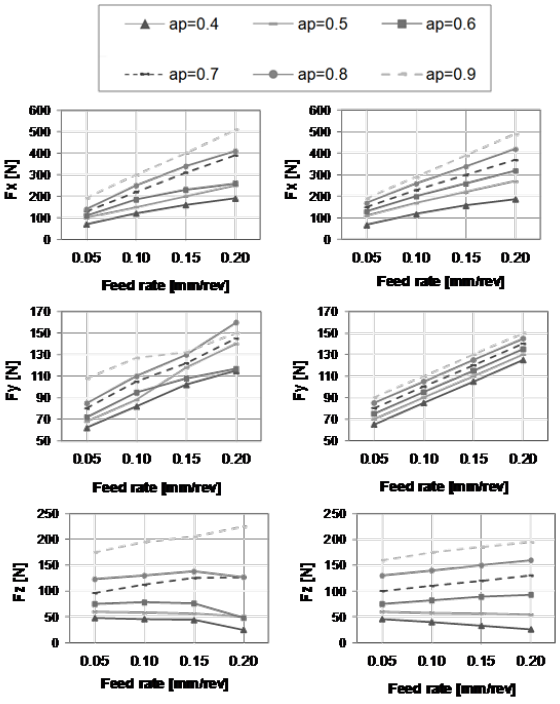

Figure 4: Experimental cutting forces without the wear effect and linearization for Vc = 250 m/min.

In this way, the slope of each linearization represents the shear cutting coefficient and the Y-axis intersection point represents the cutting coefficient due to the edge force. The cutting coefficients at the two cutting speeds show a linear tendency as the depth of cut increases, see Figure 5.

The resulting equations for describing the cutting coefficients are shown in Table 1 and Table 2. From these equations is possible to make a semi-analytical prediction of the forces without consider the wear effect. These predictions show a good agreement with experimental data

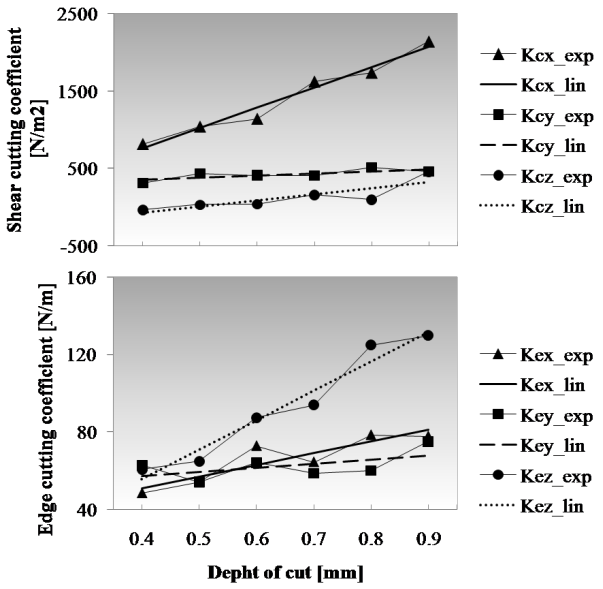

Figure 5: Experimental linearized cutting coefficients: shear cutting coefficients (up) in [N/m] and edge coefficients (down) in [N].

(see Figure 4 the correspondence between simulated and experimental ones).

Table 1: Shear cutting coefficient functions. Dependence on the depth of cut.

Shear cutting coefficient
$K_{cx} = 2628.5 \cdot a_p - 296.5$
$K_{cy} = 276.6 \cdot a_p + 241.5$
$K_{cz} = 797.1 \cdot a_p - 391.2$

Table 2: Edge cutting coefficient functions. Dependence on the depth of cut.

Edge cutting coefficient
$K_{ex} = 60.4 \cdot a_p + 26.8$
$K_{ey} = 21.2 \cdot a_p + 48.7$
$K_{ez} = 152.0 \cdot a_p - 5.3$

An example of prediction for the cutting force, using the expressions described above, is illustrated in Figure 6.

In this case, a straight cylindrical turning operation is carried out with $ap = 0.6$ mm and the selected tool geometry (CNGN, rhombic geometry with $\kappa_r = 93°$) leads to a more pronounced increment of the cutting force in the tangential direction (cutting speed direction) and in the

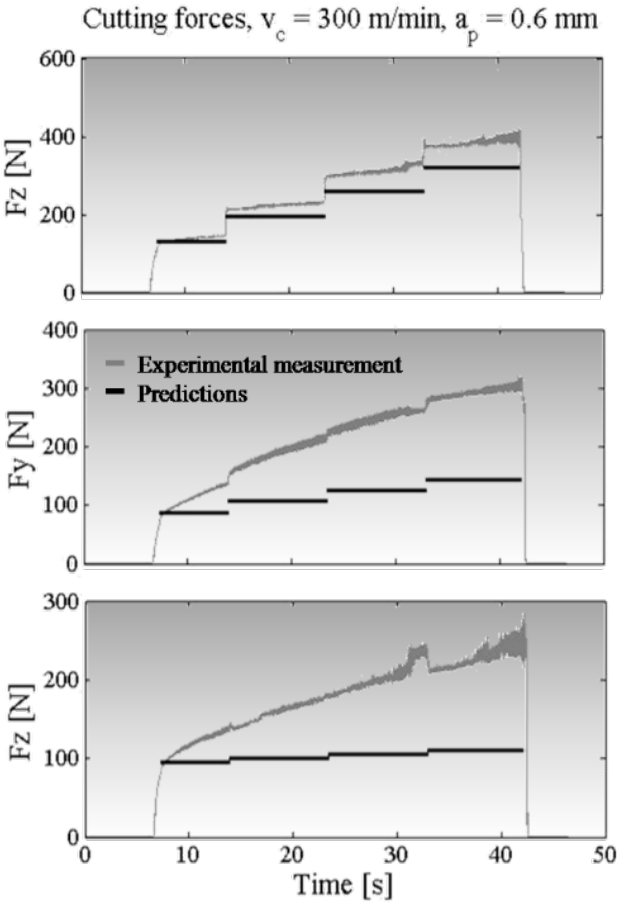

Figure 6: Force prediction neglecting the wear effect.

radial direction (Y direction) than in Z direction. This is the main reason for the small effect on the force in axial direction, if wear is not considered (Figure 6, down). It is evident that the consideration of the wear effect over the force would improve the accuracy between experimental data and predictions. This is a key issue when cutting low-machinability materials with ceramic inserts resulting in an accumulative effect over the forces. The proposed treatment for the computation of wear effects will be discussed in the next section.

5 Wear force analysis

In the scientific literature, cutting forces are often decomposed into pure (shear) cutting forces and friction or edge forces if wear is not studied. It is reasonable to consider that wear and edge forces are both due to friction mechanisms between the tool and workpiece. However, especially when machining Inconel, wear mechanisms will affect edge force components (also shear cutting compo-

nents) because the tool continuously loses material and so, the edge geometry continuously changes with respect to its theoretical profile. Under this approach, these effects were absorbed by the wear component, *i.e.*, the one that changes against time. In other words, the linearization of the cutting and friction components was done prior to wear analysis, because wear is time varying and needs a different treatment. So, cutting and edge components are considered stationary (constant) phenomena while evolving phenomena will be packaged inside the wear coefficient.

Figure 6 shows a relative distortion between the real cutting forces and the predicted ones without considering tool wear. This slope due to the wear effect is constant along each feed rate but slightly varies from one to another. Let K_w be the ratio between increasing force and time and Δt_1 the length for the first feed rate. From Equation (7), it can be said that the force at the beginning of the first feed rate could be expressed as:

$$F_{1,st} = K_c(ap) \bullet f + K_e(ap) \tag{8}$$

Then, considering the effect of wear, the force at the end of the first feed rate is defined by:

$$F_{1,end}(\Delta_{t,1}) = F_{1,st} + K_w(Vc/Vf)\Delta t_1 \tag{9}$$

where, K_w is the wear coefficient to determine the effect in the force in N/s. Thus, under the consideration that there is not significant wear in the transitions between feed rates, the force at the beginning of the second feed rate is:

$$F_{2,st} = F_{1,end} + \Delta 1 \tag{10}$$

The same approach can be extended to predict the total force as dependent on time, because wear effect causes an increasing effect on the cutting force.

The analysis to obtain the wear coefficients for the time dependent term in equation (7) uses a linear approach as well, as it was explained for K_c and K_e coefficients. The analysis finds the relationship between the slope force-time as dependent on the depth of cut. The expressions to describe this wear coefficient are in Table 3.

The force thus obtained, considering the effects of the cutting process as well as the effect introduced by wear as tool life decreases, is shown in Figure 7. Here, it is clearly denoted the matching between experimental measurements and force predictions.

At the view of Figure 7, a machinist could establish a threshold value for considering the tool replacement, allowing programmers to foretell turning force components at different wear stages. The tool life is very short when ceramics are used at 300-400 m/min, so estimation is useful for work preparation. For instance, Figure 8 shows the state of two tools after experiments in Figure 7, for 250 and 300 m/min respectively. Notch wear is disregarded when flank wear is determined.

6 Wear effects on stability

Unfortunately, tool wear cannot be neglected when machining difficult-to-cut alloys. The quality of machined parts is affected by changing conditions at the chip-tool interface. Changes in tool geometry will have drastic con-

Table 3: The wear coefficient functions depending on depth of cut.

Wear cutting coefficient	
V_c = 250 m/min	V_c = 300 m/min
$K_{wx} = 0.1474 \cdot a_p + 0.4338$	
$K_{wy} = 0.3850 \cdot a_p + 0.7763$	
$K_{wz} = 0.6226 \cdot a_p + 0.5504$	$K_{wx} = 0.1987 \cdot a_p + 0.5845$
$K_{wy} = 0.6186 \cdot a_p + 1.2475$	
$K_{wz} = 0.9714 \cdot a_p + 0.8589$	

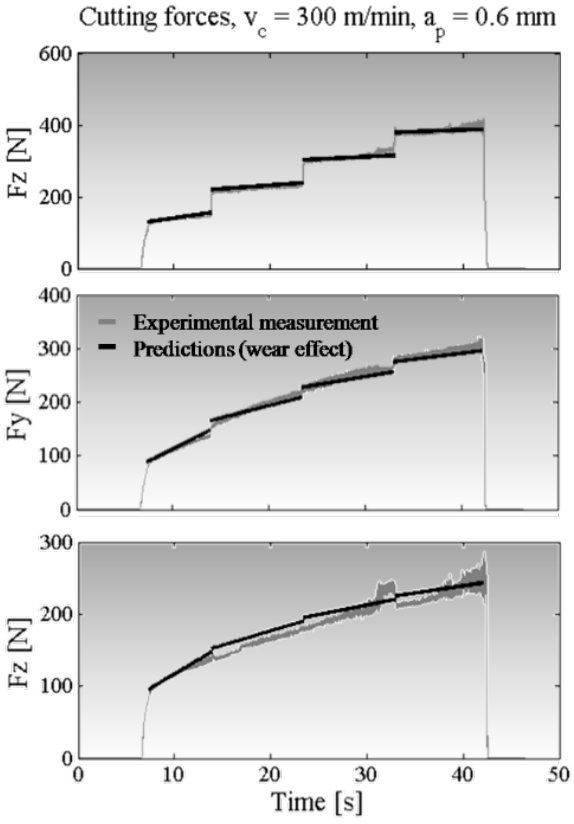

Figure 7: Force prediction considering the wear effect.

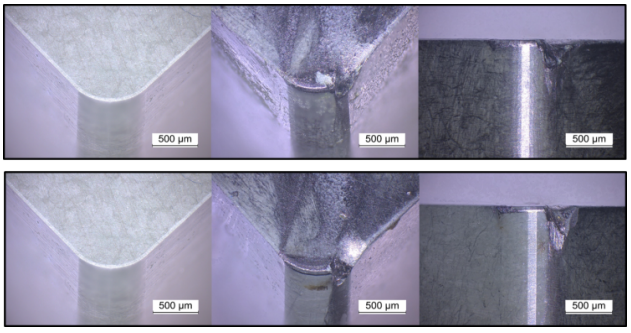

Figure 8: Tool wear of Al2O3+SiCw: new and worn tool (rake and relief faces views), at 250 m/min (up row) and 300 m/min (down row).

Table 4: Cutting coefficients at different stages of tool wear.

t = 0s	t = 15s	t = 30s
K_{cx} = 1,018 N/mm^2	K_{cx} = 1,170 N/mm^2	K_{cx} = 1,322 N/mm^2
K_{cy} = 380 N/mm^2	K_{cy} = 670 N/mm^2	K_{cy} = 961 N/mm^2
K_{cz} = 7.5 N/mm^2	K_{cz} = 266 N/mm^2	K_{cz} = 525 N/mm^2

sequences on the dynamics of the cutting process. First, cutting coefficients rapidly increase leading to lower admissible depths of cut. However, tool wear has also positive effects at low cutting speeds, where *process damping* tends to increase the available free chatter zones [37]. On the side of monitoring, many authors in the literature pointed towards the importance of recording the vibration (acceleration) signal [38, 39]. These approaches need further improvements in order to be reliable solutions.

On the side of modelling, we present some stability lobes considering tool wear from the corresponding dynamic turning model. The above expressions for the specific cutting energy were introduced in the chatter model presented in [40–42]. The Chebyshev collocation method (CCM) was used with meshes of 200x150 and 250 discretization points and the tested modal parameters were: f_n = 711.75 Hz, k = 1e7 N/m, m = 0.5 kg, ξ = 0.01. A tool with κr = 45° angle, similar to round inserts, is assumed. The cutting coefficients considering tool degradation over time were calculated at times t = 0 (new), 15 and 30 s (Table 4) using ap = 0.5 mm and f = 0.1 mm/rev.

Figure 9 shows how important is keeping tool wear under control to avoid chatter. It significantly decreases the chatter free zones in a few seconds what is particularly risky in aerospace industry when turning expensive parts. Additionally, when combining worn tools and low

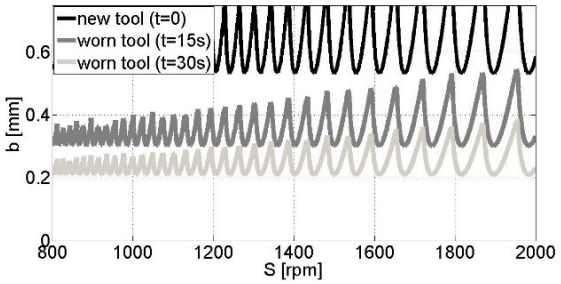

Figure 9: Stability lobes considering tool wear.

spindle speeds (for instance, in turning or boring) it is important considering that process damping effect could appear. This phenomenon tends to increase the stability zone and is relatively easily to consider within the model. However, it depends on a number of parameters (tool geometry, preparation, cutting parameters and modal parameters) and it is difficult to obtain experimentally.

7 Conclusions

The cutting force prediction has been always a subject of concern in the planning of turning operations in Inconel 718 with ceramic inserts. The estimation could help machinist to program tool replace or reduce the risks in cases of thin-wall parts machining.

This study presents a predictive model to obtain the three force components in the straight turning process, based on a linearization of the tool wear progression. This linearization lies in the slope observed during the experiments performed at several cutting speeds. Because of the aggressive cutting of ceramics on superalloys causing high temperatures and stresses, flank wear effect need to be included in the force prediction. In fact, the weight of the wear component into the total force seems to be so variable that estimation cannot be achieved without considering the ploughing effects caused by tool corner chamfering due to wear.

This work proposes a model that considers the wear coefficients deviation with the depth of cut, offering a set of equations for different cutting speeds. Similar relationships are found for cutting and edge coefficients. The effects of feed rate are included for the cutting and wear terms in the general expressions (for equation (8) and for equation (9)).

Therefore, model makes possible for given cutting conditions to predict turning force components at a certain time. The model achieved has been adjusted in the width

range from V_c = 250 to 300 m/min, typical for the application of Al_2O_3+SiCw ceramic tools in Inconel 718.

The so proposed model can help to obtain forces or being part of a complex dynamic model.

Acknowledgement: We are grateful to research projects TURBO from MINECO, project INNPACTO DESAFIO II by MINECO as well, initiative ZABALDUZ, and UPV/EHU number UFI 11/29.

Nomenclature

κr	cutting edge approach angle in °
ξ	damping ratio
ap	depth of cut in mm
f	feed per revolution in mm/rev
f_n	mode frequency in Hz
k	modal stiffness in N/m
K_{cx}	shear cutting coefficient in N/mm^2
K_{ex}	specific edge force in N/mm
K_{wx}	specific edge wear force in N/s
m	mass
V_B	flank wear in mm
Vc	cutting speed in m/min
Vf	linear feed rate in mm/min

References

[1] Suarez A, López de Lacalle, L.N., Polvorosa, R., Veiga F., Wretland, A., Effects of high-pressure cooling on the wear patterns Wear-dependent specific coefficients in a mechanistic model on turning inserts used on alloy IN718, Mat. Manuf. Proc., 2016,32, 6.

[2] Suárez A., Veiga F., López de Lacalle L.N., Polvorosa R., Lutze S., Wretland A., Effects of Ultrasonics-Assisted Face Milling on Surface Integrity and Fatigue Life of Ni-Alloy 718, J. Mat. Eng. Perf.

[3] Narutaki N., Yamane Y., Hayashi K., Kitagawa T., High speed machining of Inconel 718 with ceramic tools, Annals of CIRP, 1993, 42, 103-106.

[4] Dudzinski D., Devillez A.,Moufki A., Larrouqučre D., Zerrouki V., Vigneau J., A review of developments towards dry and high speedmachining of Inconel 718 alloy, Int. J.Mach. ToolsManuf., 2004, 44, 439-456.

[5] Fang N., Wu Q., A comparative study of the cutting forces in high speedmachining of Ti-6Al-4V and Inconel 718 with a round cutting edge tool, J. Mat. Proc. Tech., 2009, 209, 4386-4389.

[6] Thakur D.G., Ramamoorthy B., Vijayaraghavan L., Study on the machinability characteristics of superalloy Inconel 718 during high speed turning, Mat. Des., 2009, 30, 1718-1725.

[7] Kothamasu R., Huang S.H., Verduin,W.H., Comparison of computational intelligence and statistical methods in condition monitoring for hard turning, Int. J. Prod. Res., 2005, 43(3), 597-610.

[8] Kountanya R., Surface finish and tool wear characterization in hard turning using a mathematical cutting tool representation, Mach. Sci. Tech., 2011, 15(4), 429-452.

[9] Bartary G., Choudhury S.K., State of the art in hard turning, Int. J. Mach. Tools Manuf., 2012, 53(1), 1-14.

[10] Saini S., Ahuja I.S., Sharma V.S., Residual Stresses, surface roughness, and tool wear in hard turning: A comprehensive review, Mat. Manuf. Proc., 2012, 27(6), 583-598.

[11] Arunachalam R.M., Mannam M.A., Spowage A.C., Residual stress and surface roughness when facing age hardened Inconel 718 with CBN and ceramic cutting tools, Int. J.Mach. Tools Manuf., 2004, 44, 879-887.

[12] Arunachalam R.M., Mannan M.A., Performance of CBN cutting tools in facing of age hardened Inconel 718, Trans. NAMRI/SME, XXXII, 2004.

[13] Cui X., Guo J., Zheng J., Optimization of geometry parameters for ceramic cutting tools in intermittent turning of hardened steel, Mat. Des., 2016, 92(15), 424-437.

[14] Xu K., Zou B., Huang C., Yao Y., Zhou H., Li Z., Machinability of Hastelloy C-276 using Hot-pressed sintered Ti(C7N3)-based cermet cutting tools, Chin. J. Mech. Eng., 2015, 28(3), 599-606.

[15] Yan S., Zhu D., Zhuang K., Zhang X., Ding H., Modelling and analysis of coated tool temperature variation in dry milling of Inconel 718 turbine blade considering flank wear effect, J. Mat. Proc. Tech., 2014, 214(12), 2985-3001.

[16] Yun J.Y., Shin G.S., Kim D.I., Lee H.S., Kang W.S., Kim S.J., 2015, Effect of carbide size and spacing on the fretting wear behaviour of Inconel 690 SG tube mated with SUS 409, Wear, 2015, 338–339(15), 252-257.

[17] Mi X., Wang W.X., Xiong X.M., Qian H., Tang L.C., Xie Y.C., Peng J.F., Cai Z.B., Zhu M.H., Investigation of fretting wear behaviour of Inconel 690 alloy in tube/plate contact configuration, Wear, 2015, 328–329(15), 582-590.

[18] Fernández-Valdivielso A., López de Lacalle L.N., Urbikain G., Rodriguez A., Detecting the key geometrical features and grades of carbide inserts for the turning of nickel-based alloys concerning surface integrity, Proc. Inst. Mech. Eng. Part C, J. Mech. Eng. Sci., 2015, 1-8.

[19] Ezugwu E.O., Bonney J., Effect of high-pressure coolant supply when machining nickel-base, Inconel 718, alloy with coated carbide tools, J. Mat. Process. Technol., 2004, 153–154, 1045–1050.

[20] Vagnorius Z., Sřrby K., Effect of high-pressure cooling on life of SiAlON tools in machining of Inconel 718, Int. J. Adv. Manuf. Tech., 2011, 54(1), 83-92.

[21] Wei W., Xu J., Fu Y., Yang S., Tool wear in turning of titanium alloy after thermohydrogen treatment, Chin. J. Mech. Eng., 2012, 25(4), 776-780.

[22] Jomaa W., Songmene V., Bocher P., Surface Finish and Residual Stresses Induced by Orthogonal Dry Machining of AA7075- T651. Mat., 2014, 7(3), 1603-1624.

[23] López de Lacalle L.N., Sánchez J.A., Lamikiz A., Celaya A. Plasma assisted milling of heat-resistant superalloys, Trans. ASME, J. Manuf. Sci. Eng., 2004, 126, 274-285.

[24] Olovsjö S., Wretland A., Sjöberg G., The effect of grain size and hardness of Waspaloy on the wear of cemented carbid tools. Int. J. Adv. Manuf. Tech., 2010, 50(9), 907-915.

[25] Liu P., Xu J.H., Fu Y.C., Cutting force and its frequency spectrum characteristics in high speed milling of titanium alloy with a polycrystalline diamond tool, J. Zhejiang University Science A, 2011, 12(1), 56-62.
[26] Altintas Y., Budak E., Analytical Prediction of Stability Lobes in Milling, Annals CIRP Manuf. Tech., 1995, 44, 357-362.
[27] Urbikain G., Artetxe E., López de Lacalle L.N., Numerical simulation of milling forces with barrel-shaped tools considering run out and tool inclination angles, Appl. Math. Mod., 2017, 47, 619–636.
[28] Altintas Y., Manufacturing Automation, Cambridge University Press, 2000.
[29] Kobayashi S., Thomsen E.G., The role of friction in metal cutting, J. Eng. Ind., 1960, 82, 324.
[30] Thomsen E.G., Macdonald A.G., Kobayashi S., Flank friction studies with carbide tools reveal sublayer plastic flow, J. Eng. Ind., 1962, 84, 53.
[31] Zorev N.N., Metal cutting mechanics, First Edition, 1966, Oxford: Pergamon Press. pp. 526.
[32] Elbestawi M.A., Ismali F., Du R.X., Ullagaddi B.C., 1991, Modelling machining dynamics including damping in the tool work piece interface, Tribol. Asp. Manuf., 1991, 54, 253-258.
[33] Wu D.W., Application of a comprehensive dynamic cutting force model to orthogonal wave generating processes, Int. J. Mech. Sci., 1988, 30, 581-660.
[34] Challen J.M., Oxley P.L.B., An explanation of the different regimes of friction and wear using asperity deformation models, Wear, 1979, 53, 229-243.
[35] Waldorf D.J., DeVor R.E., Kappor S.G., A slip-line field for ploughing during orthogonal cutting, ASME. J. Manufacturing Sci. Eng., 1998, 120, 693-699.
[36] Park K.H., Yang G.D., Le D.Y., Tool wear analysis on coated and uncoated carbide tools in inconel machining, Int. J. Prec. Eng. Manuf., 2015, 16(7), 1639-1645.
[37] Altintas Y., Eynian M., Onozuka, H., Identification of dynamic cutting force coefficients and chatter stability with process damping, CIRP Annals – Manuf. Tech., 2008, 57(1), 371-374.
[38] Chiou R.Y., Liang S.Y., Analysis of acoustic emission in chatter vibration with tool wear effect in turning, Int. J. Mach. Tools Manuf., 2000, 927-941.
[39] Lim G.H., Tool-wear monitoring in machining turning, J. of Mat. Proc. Tech., 1995, 51, 25-36.
[40] Urbikain G., López de Lacalle L.N., Fernández-Valdivielso A., Regenerative vibration avoidance due to tool tangential dynamics in interrupted turning, J. Sound Vib., 2014, 333(17), 3996–4006.
[41] Urbikain G., Olvera D., López de Lacalle L.N., Elías-Zúñiga A., Stability and vibrational behaviour in turning processes with low rotational speeds, Int. J. Adv. Manuf. Tech., 2015, 80, 871–885.
[42] Urbikain G., López de Lacalle L.N., Training and learning of specialised engineers bymeans of a new advanced software,Comp. Appl. Eng. Edu.